UNIVERSITA' DEGLI STUDI DI MILANO BICOCCA

FACOLTA' DI SCIENZE MATEMATICHE, FISICHE E NATURALI
DIPARTIMENTO DI FISICA "GIUSEPPE OCCHIALINI"
ACADEMIC YEAR 2022-2023

Essay for the Computational Physics Laboratory exam

Quantum harmonic oscillator on the lattice

Abstract

The purpose of this work is to simulate a quantum harmonic oscillator on a discrete time lattice with periodic boundary conditions, using the path integral approach, exploiting the Monte Carlo method of importance sampling. We are able to extract the square of the matrix element of the position operator between the vacuum and the first excited state and the energy gap between the same states in the discrete. Physical observables in the continuum are extrapolated through a fit of the results obtained at fixed lattice spacing.

Professor: Leonardo Giusti
Student: Federico De Matteis

Contents

1 Theoretical preliminaries

This section has the aim of giving an overview of the framework and methods used in this work, introducing formulas that will be used to extract physical informations from lattice simulations.

1.1 The harmonic oscillator

In the continuum the quantum harmonic oscillator is described by the Hamiltonian

$$\hat{\mathrm{H}} = \frac{\hat{p}^2}{2m} + \frac{1}{2}m\omega^2\hat{x}^2, \tag{1.1.1}$$

whose eigenvalues are given by $\mathrm{E}_n = \omega(n + \frac{1}{2})$ and whose eigenfunctions $|\mathrm{E}_n\rangle$ satisfy the eigenvalues equation for the parity operator:

$$\hat{\mathrm{P}}|\mathrm{E}_n\rangle = (-1)^n|\mathrm{E}_n(x)\rangle. \tag{1.1.2}$$

In this work, We are also interested in the matrix elements that are given below:

$$\begin{aligned} \langle \mathrm{E}_0|\hat{x}|\mathrm{E}_1\rangle &= \frac{1}{\sqrt{2m\omega}}, \\ \langle \mathrm{E}_0|\hat{x}|\mathrm{E}_0\rangle &= 0, \\ \langle \mathrm{E}_0|\hat{x}^2|\mathrm{E}_0\rangle &= \frac{1}{2m\omega}. \end{aligned} \tag{1.1.3}$$

1.2 Euclidean path integral

The path integral for the quantized theory is defined in discretized Euclidean time as:

$$\mathrm{Z}_{\mathtt{a}}(\mathrm{T}) = \left(\frac{m}{2\pi\mathtt{a}}\right)^{\frac{\mathrm{N}}{2}} \int \prod_{\mathtt{i}=0}^{\mathrm{N}-1} dx_{\mathtt{i}} e^{-\mathcal{S}_{\mathrm{E}}} = \mathrm{Tr}[\hat{\mathrm{T}}_{\mathtt{a}}^{\mathrm{N}}]. \tag{1.2.1}$$

The operator $\hat{\mathrm{T}}_{\mathtt{a}}$ is the euclidean transfer operator which will be introduced in the next subsection. In order to work in the path integral formalism We define a periodic time lattice of length $\mathrm{T} = \mathrm{N}\mathtt{a}$ where $\mathtt{a}$ is the lattice spacing and N is the number of points in the lattice. The $\mathtt{k}$-th instant in Euclidean time is then given by $\mathtt{t}_{\mathtt{k}} = \mathtt{k}\mathtt{a}$ with $\mathtt{k} = 0, ..., \mathrm{N}-1$. The action describing the dynamics of the harmonic oscillator on the lattice in the Euclidean formalism is:

$$\mathcal{S}_{\mathrm{E}} = \mathtt{a}\sum_{\mathtt{t}=0}^{\mathrm{N}-1}\left\{\frac{m}{2}\left(\frac{x_{\mathtt{t}+1} - x_{\mathtt{t}}}{\mathtt{a}}\right)^2 + \frac{m\omega^2}{2}x_{\mathtt{t}}^2\right\}. \tag{1.2.2}$$

In this context, the Euclidean transfer operator is given by:

$$\hat{\mathrm{T}}_{\mathtt{a}} = e^{-\frac{\mathtt{a}}{2}\hat{\mathrm{V}}(\hat{x})}e^{-\mathtt{a}\frac{\hat{p}^2}{2m}}e^{-\frac{\mathtt{a}}{2}\hat{\mathrm{V}}(\hat{x})} \tag{1.2.3}$$

that is, the operator that evolves the system by one time step $\delta t = a$. As unitary, it can be written as the exponential of an Hermitian operator $\hat{\tilde{H}}$ such that:

$$\hat{T}_a = e^{-a\hat{\tilde{H}}} = e^{-a\hat{H}+O(a^2)}. \tag{1.2.4}$$

The eigenvalues of the transfer operator associated with its eigenfunctions $|\tilde{E}_n\rangle$ are given by:

$$\hat{T}_a|\tilde{E}_n\rangle = e^{-a\tilde{E}_n}|\tilde{E}_n\rangle. \tag{1.2.5}$$

1.3 Spectrum of the transfer operator

We introduce the Hamiltonian $\hat{H}_D$ of an auxiliary harmonic system that has the same expression as the Hamiltonian of the continuum in Eq. (1.1.1) but with pulsation $\bar{\omega}$ given by:

$$\bar{\omega}^2 = \omega^2\left(1 + \frac{a^2\omega^2}{4}\right), \tag{1.3.1}$$

which the depends on a and differs from ω of the continuum by discretization errors $O(a^2)$. The auxiliary Hamiltonian operator just introduced satisfies the commutation relation:

$$\left[\hat{T}_a, \hat{H}_D\right] = 0. \tag{1.3.2}$$

Therefore, since $\hat{H}_D$ is diagonalizable and its spectrum is non-degenerate, $\hat{H}_D$ and $\hat{T}_a$ share the same eigenfunctions $|\tilde{E}_n\rangle$. The eigenvalues of the euclidean transfer operator are given by Eq. (1.2.5) with $\tilde{E}_n = \tilde{\omega}(n + \frac{1}{2})$ where $\tilde{\omega}$ is related to ω and $\bar{\omega}$ through the relation:

$$\tilde{\omega} = \frac{1}{a}\log\left(1 + a\bar{\omega} + \frac{a\omega^2}{2}\right). \tag{1.3.3}$$

$\hat{H}_D$ has the same eigenfunctions as the Hamiltonian of the continuum $\hat{H}$, with the only prescription of making the substitution $\omega \to \bar{\omega}$. In particular $|\tilde{E}_n\rangle$ are still eigenstates of the parity operator $\hat{P}$[1] and generic matrix elements between eigenstates of $\hat{H}_D$ (and so of $\hat{T}_a$) have the same structure as in the continuous case. For instance, We are interested in the matrix element:

$$\langle\tilde{E}_0|\hat{x}|\tilde{E}_1\rangle = \frac{1}{\sqrt{2m\bar{\omega}}}. \tag{1.3.4}$$

Notice that eigenvalues and matrix elements computed above tend to the standard definitions of the continuum in the limit of $a \to 0$, indeed $\bar{\omega} = \omega + O(a^2)$[2]; nonetheless their discretization errors are different. To summarize, the description above introduces explicit formulas for the eigenvalues and eigenstates of the euclidean transfer operator at a fixed lattice spacing a, providing a tool to check the numerical quantities which We will compute from simulations, as discussed in section 1.5 ("Observables").

[1] This property will be used in the next section.

[2] The expansion in the limit of $a \to 0$ is given in (4.0.1)

1.4 Two point correlation function

The object from which physical informations about the system will be extracted is the two-point correlation function $\langle x_{\mathtt{l}} x_{\mathtt{k}} \rangle$, which is written in the path integral formalism as:

$$\langle x_{\mathtt{l}} x_{\mathtt{k}} \rangle = \frac{\left(\frac{m}{2\pi \mathtt{a}}\right)^{\frac{\mathrm{N}}{2}}}{\mathrm{Z}_{\mathtt{a}}(\mathrm{T})} \int \prod_{i=0}^{\mathrm{N}-1} dx_i e^{-\mathcal{S}_{\mathrm{E}}} x_{\mathtt{l}} x_{\mathtt{k}}. \tag{1.4.1}$$

The correlation function in (1.4.1) can be also written using the operator formalism:

$$\langle x_{\mathtt{l}} x_{\mathtt{k}} \rangle = \frac{1}{\mathrm{Tr}[\hat{\mathrm{T}}_{\mathtt{a}}^{\mathrm{N}}]} \mathrm{Tr}[\hat{\mathrm{T}}_{\mathtt{a}}^{\mathrm{N}-|\mathtt{l}-\mathtt{k}|} \hat{x} \hat{\mathrm{T}}_{\mathtt{a}}^{|\mathtt{l}-\mathtt{k}|} \hat{x}]. \tag{1.4.2}$$

By carrying out the computation of the traces in Eq. (1.4.2) and taking the limit for $\mathrm{T} \to \infty$ at fixed lattice spacing $\mathtt{a}$, We are left with the leading contributions:

$$\langle x_{\mathtt{l}} x_{\mathtt{k}} \rangle \simeq \frac{1}{e^{-\mathtt{a}\tilde{\mathrm{E}}_0 \mathrm{N}}} \left(e^{-(\mathrm{N}-|\mathtt{l}-\mathtt{k}|)\mathtt{a}\tilde{\mathrm{E}}_0} e^{-|\mathtt{l}-\mathtt{k}|\mathtt{a}\tilde{\mathrm{E}}_1} + e^{-(\mathrm{N}-|\mathtt{l}-\mathtt{k}|)\mathtt{a}\tilde{\mathrm{E}}_1} e^{-|\mathtt{l}-\mathtt{k}|\mathtt{a}\tilde{\mathrm{E}}_0} \right) |\langle \tilde{\mathrm{E}}_0 | \hat{x} | \tilde{\mathrm{E}}_1 \rangle|^2, \tag{1.4.3}$$

since by parity the first nonzero contributions are those involving the matrix element between $|\tilde{\mathrm{E}}_0\rangle$ and $|\tilde{\mathrm{E}}_1\rangle$. Finally, the last equation can be re-arranged to obtain:

$$\langle x_{\mathtt{l}} x_{\mathtt{k}} \rangle \simeq 2\cosh \left[\mathtt{a}(\tilde{\mathrm{E}}_1 - \tilde{\mathrm{E}}_0) \left(\frac{\mathrm{N}}{2} - |\mathtt{l}-\mathtt{k}| \right) \right] e^{-\mathtt{a}\frac{\mathrm{N}}{2}(\tilde{\mathrm{E}}_1 - \tilde{\mathrm{E}}_0)} |\langle \tilde{\mathrm{E}}_0 | \hat{x} | \tilde{\mathrm{E}}_1 \rangle|^2. \tag{1.4.4}$$

We can expand the correlator in the region $\frac{\mathrm{N}}{2} \ll |\mathtt{l}-\mathtt{k}|$ as:

$$\langle x_{\mathtt{l}} x_{\mathtt{k}} \rangle \simeq |\langle \tilde{\mathrm{E}}_0 | \hat{x} | \tilde{\mathrm{E}}_1 \rangle|^2 e^{-\mathtt{a}|\mathtt{l}-\mathtt{k}|(\tilde{\mathrm{E}}_1 - \tilde{\mathrm{E}}_0)}; \tag{1.4.5}$$

thus the correlator decrease exponentially with increasing $|\mathtt{l}-\mathtt{k}|$ (remaining in the region $|\mathtt{l}-\mathtt{k}| \ll \frac{\mathrm{N}}{2}$).

1.5 Observables

The formula (1.4.4) makes clear the symmetry of the correlation function around $\frac{\mathrm{N}}{2}$, so, from now on We are interested in the values of the correlator for $\mathtt{t} = 1, ..., \frac{\mathrm{N}}{2} - 1$. Since $\langle x_{\mathtt{l}} x_{\mathtt{k}} \rangle$ depends on $\mathtt{l}$ and $\mathtt{k}$ only through their difference, We write $\mathtt{a}|\mathtt{l}-\mathtt{k}| = \mathtt{t}$ and use the definition $\langle x_{\mathtt{k}} x_{\mathtt{k}+t} \rangle = C(\mathtt{t})$ henceforth; also for convenience, We use the notation $\tilde{\mathrm{E}}_1 - \tilde{\mathrm{E}}_0 = \Delta\tilde{\mathrm{E}}_{01}$. Reversing the result found in Eq. (1.4.4) allows to write the formula for the energy gap:

$$\Delta\tilde{\mathrm{E}}_{01}(\mathtt{t}) = \frac{1}{\mathtt{a}} \mathrm{acosh} \left[\frac{C(\mathtt{t}+1) + C(\mathtt{t}-1)}{2C(\mathtt{t})} \right], \tag{1.5.1}$$

and inserting the result (1.5.1) into (1.4.4) the matrix element is explicitly written as

$$|\langle \tilde{\mathrm{E}}_0 | \hat{x} | \tilde{\mathrm{E}}_1 \rangle|^2(\mathtt{t}) = \frac{C(\mathtt{t}) e^{\frac{\mathrm{N}}{2}\mathtt{a}\Delta\tilde{\mathrm{E}}_{01}(\mathtt{t})}}{2\cosh[(\frac{\mathrm{N}}{2} - \mathtt{t})\mathtt{a}\Delta\tilde{\mathrm{E}}_{01}(\mathtt{t})]}. \tag{1.5.2}$$

In section 3 ("Physics results") we will use the notation $|\tilde{x}_{01}|^2$ to indicate the matrix element. Quantities in Eqs. (1.5.1) and (1.5.2) are precisely the physical observables that are intended to be computed in this work and will be compared with the discrete theoretical results in Eqs. (1.3.3) and (1.3.4). The physical observables will be computed on different lattices, at fixed lattice spacing, then We will take the limit of $\mathtt{a} \to 0$ and extract the physical observables in the continuum.

2 Monte Carlo implementation

In order to compute the multidimensional integral in Eq. (1.4.1) the importance sampling Monte Carlo method is used; this is able to provide a probabilistic estimate of the correlator by extracting M N-tuple configurations of coordinates $x_0, ..., x_{N-1}$ distributed according to the p.d.f. given by $\frac{e^{-S_E}}{Z_a(T)}$. By the central limit theorem, the estimate of the integral in Eq. (1.4.1) is given, in the limit of large M, by the random variable

$$\bar{C}(\mathtt{t}) = \frac{1}{M} \sum_{\mathtt{j}=0}^{M-1} C_{\mathtt{j}}(\mathtt{t}), \tag{2.0.1}$$

where $C_{\mathtt{j}}(\mathtt{t}) = (x_{\mathtt{l}})_{\mathtt{j}}(x_{\mathtt{k}})_{\mathtt{j}}$; in sub-section 2.3 we will use a different definition for $C_{\mathtt{j}}(\mathtt{t})$ in which We will average over all possible combinations of coordinates that has the same distance in the physical time. The error on the estimation of the integral is given by:

$$\sigma(\bar{C}(\mathtt{t})) = \frac{\sigma(C(\mathtt{t}))}{\sqrt{M}}. \tag{2.0.2}$$

The fundamental difference between MC methods and exact numerical methods (such as Gaussian quadrature or the Simpson's rule) consists in the interpretation of the error on the estimation of the integral, which is of statistical nature and does not depend on the dimensionality of the integral.

2.1 Useful properties of Markov chains

Markov chains allow the extraction of N-tuples with the desired probability distribution. An ergodic Markov chain is introduced, defined by the transition matrix $P_{\mathtt{i},\mathtt{j}}$, i.e. the matrix having as components the transition probabilities from a state $\mathtt{i}$ to a state $\mathtt{j}$ of the chain. By the Ergodic Theorem for such a chain there exists well-defined the limit

$$\lim_{N\to\infty} P^N_{\mathtt{i},\mathtt{j}}; \tag{2.1.1}$$

such a limit does not depend on the starting state $\mathtt{j}$ of the random walk on the chain. We introduce now a probability distribution:

$$p_{\mathtt{i}} = \frac{r_{\mathtt{i}}}{\sum_{\mathtt{i}} r_{\mathtt{i}}} \geq 0, \quad r_{\mathtt{i}} \geq 0 \quad \forall \mathtt{i}. \tag{2.1.2}$$

If the ergodic Markov chain introduced above satisfies the detailed balance condition:

$$r_{\mathtt{i}} P_{\mathtt{i},\mathtt{j}} = r_{\mathtt{j}} P_{\mathtt{j},\mathtt{i}}, \tag{2.1.3}$$

then it holds that $p_{\mathtt{i}}$ is given by the limit (2.1.1). In the limit of large N the chain "extracts" random variables with the probability distribution given by $p_{\mathtt{i}}$.

2.2 The Metropolis algorithm

Let us introduce a transition probability $\mathrm{Q}_{\mathtt{i},\mathtt{j}}$ that satisfies the microreversibility condition:

$$\mathrm{Q}_{\mathtt{i},\mathtt{j}} = \mathrm{Q}_{\mathtt{j},\mathtt{i}} \qquad \forall \mathtt{i},\mathtt{j}, \tag{2.2.1}$$

that is, the transition probability from state `i` to state `j` is equal to the transition probability from `j` to `i`. Under these assumption, We can draw a Markov chain described by the transition matrix:

$$\mathrm{P}_{\mathtt{i},\mathtt{j}} = \left\{ \begin{array}{ll} \mathrm{Q}_{\mathtt{i},\mathtt{j}} & \text{if } \frac{r_{\mathtt{j}}}{r_{\mathtt{i}}} > 1 \\ \mathrm{Q}_{\mathtt{i},\mathtt{j}} \frac{r_{\mathtt{j}}}{r_{\mathtt{i}}} & \text{if } \frac{r_{\mathtt{j}}}{r_{\mathtt{i}}} < 1 \end{array} \right\}. \tag{2.2.2}$$

This transition matrix identifies a Markov chain for which the detailed balance condition in Eq. (2.1.3) holds, and therefore, in the limit $\mathrm{N} \to \infty$, it extracts states with the asymptotic probability $p_{\mathtt{i}}$ in Eq. (2.1.2). The procedure just explained goes under the name of "Metropolis algorithm"(MA).

In this work the MA is implemented using the asymptotic distribution $p_{\mathtt{i}} = \frac{e^{-\mathcal{S}_{\mathrm{E}}}}{\mathrm{Z}_{\mathtt{a}}(\mathrm{T})}$. In order to do so We initialize the N-tuple $x_{\mathtt{i}}$[3], where $\mathtt{i} = \{0, ..., \mathrm{N}-1\}$ are the positions of the particle at the time slice $\mathtt{t}_{\mathtt{i}}$, and We consider one by one the components of the path; a new value for $x_{\mathtt{i}}$ is proposed using as $\mathrm{Q}_{\mathtt{i},\mathtt{j}}$ the flat probability distribution[4] of radius Δ, which meets the condition (2.2.1). The proposed change in the coordinate of the path is given by:

$$x_{\mathtt{i}}^{new} = x_{\mathtt{i}} - 2\Delta\left(\mathrm{R}_1[\mathtt{i}] - \frac{1}{2}\right), \tag{2.2.3}$$

where Δ is a free parameter of the MA, while R_1 is a random variable extracted from the flat distribution between 0 and 1. After the proposal We estimate the variation of the action $\delta\mathcal{S}_{\mathrm{E}}$[5] due to the change in the coordinate `i` of the path and We implement the accept/reject criterion as follows:

$$\begin{array}{lll} 1)\ \text{If} & e^{-\delta\mathcal{S}_{\mathrm{E}}} > \mathrm{R}_2[\mathtt{i}] & \text{accept the proposal with } p_{\mathtt{i}} = 1 \\ 2)\ \text{If} & e^{-\delta\mathcal{S}_{\mathrm{E}}} < \mathrm{R}_2[\mathtt{i}] & \text{accept the proposal with } p_{\mathtt{i}} = e^{-\delta\mathcal{S}_{\mathrm{E}}} \end{array} \tag{2.2.4}$$

where R_2 is also a random number drawn from the flat distribution between 0 and 1. Notice that the argument `i` in $\mathrm{R}_1, \mathrm{R}_2$ stands for the components of the tuples. The procedure performed on all the elements of the N-tuple is called sweep, namely the building block of the MC procedure[6].

2.3 Thermalization of Markov chains

In the previous section the core ingredients of the MA were given. Once the chain is in the asymptotic regime the MA extracts the Feynman's paths weighting them with the Boltzmann

[3] i.e. with a null state or a random state.

[4] Using the flat randomizer implemented in the module "**ranlxd.c**".

[5] The equation used for $\delta\mathcal{S}_{\mathrm{E}}$ can be found in the appendix at (6.3.1)

[6] The sweep procedure is implemented in the module "**sweep.c**".

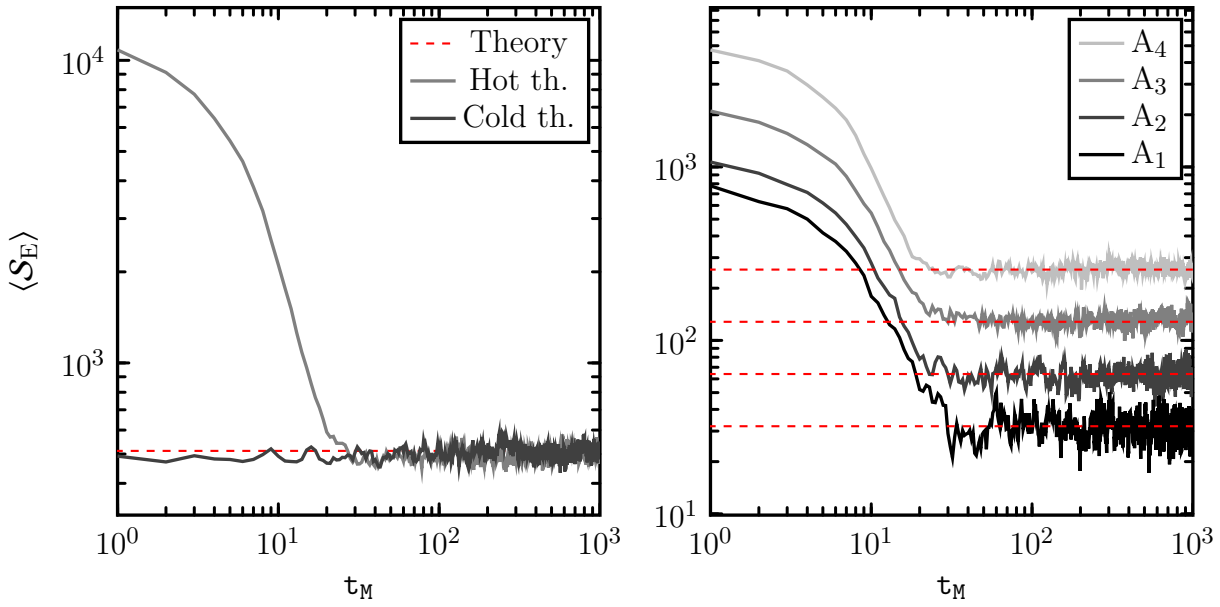

Figure 1: Left:Action for the lattice A_5 along Markov steps; the Markov chain is initialized with a random state (Hot Thermalization) and with a null state (Cold Thermalization). Right: Hot Thermalizations for the chains used for the series of lattice $\{A_1, ..., A_4\}$.

probability $\frac{e^{-\mathcal{S}}}{Z_a(T)}$, namely the chain is "thermalized". The aim of this subsection is to ensure that the Markov chains used reach the asymptotic regime, which is necessary for collecting measures in which We are interested (the correlator); to do so We use the value of $\mathcal{S}_E$ itself. We can compute the expectation value of $\mathcal{S}_E$ as a usual PI observable, it is given by:

$$\langle \mathcal{S}_E \rangle = \int \prod_{i=0}^{N-1} dx_i \; \mathcal{S}_E \; e^{-\mathcal{S}_E} \simeq \frac{N}{2}. \tag{2.3.1}$$

We expect the action to fluctuate around the value $\frac{N}{2}$ when the Markov chain is thermalized. The thermalization for the chains used is carried out by performing a large number of sweeps; at the end of each sweep the action is computed from (1.2.2), looking for a plateau region, as shown in figure 1. We name the number of Markov steps required for the thermalization of a chain as τ_{TH}.

Due to the ergodic nature of the Markov chains used, the asymptotic regime does not depend in any way on their starting states, as anticipated in section 2.1; in particular, the plot on the left in figure 1 shows that for two initializations of the path the action "thermalizes" around the value given by Eq. (2.3.1).

After the thermalization, We compute the rate of acceptance in the change of the coordinates in the Feynman's path during a single sweep and We call it "acceptancy". The acceptancy is averaged over the different sweeps in the MC and is used as an indicator of its efficiency; the acceptance rate is directly affected by Δ; using a flat distribution with an high radius Δ results indeed in a low acceptance rate, making the algorithm ineffective in path generation[7]. Once the chain is in the asymptotic regime, the primary MC variable is

[7] A more precise discussion is given in sub-section 2.4.

collected:

$$C_j(t) = \frac{1}{N}\sum_{k=0}^{N-1} x_k^j x_{k+t}^j \tag{2.3.2}$$

where N is the size of the N-tuple, while the index j runs on the number of sweeps in the MC. Again We underline that (2.3.2) differs from the definition of $C_j(t)$ used in (2.0.1), since it is an average over combinations of coordinates that has the same distance in physical time. From now on We will refer to (2.3.2) when using the notation $C_j(t)$.

2.4 Autocorrelation times

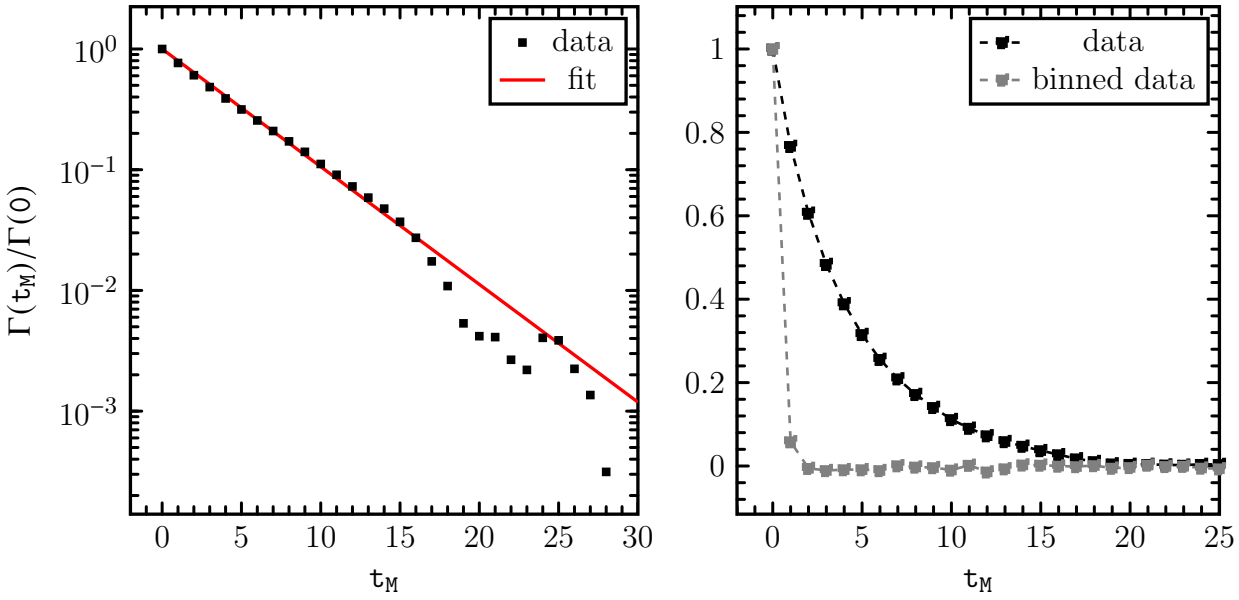

Figure 2: Left: Autocorrelation of $C_j(t)$ calculated for lattice A_1 using $\Delta = 1$ in logarithmic scale; the exponential fit is performed to extract the autocorrelation time, represented by the red line. On the right the autocorrelation is shown before and after the binning procedure. t_M stand for the Markovian time.

The variables extracted from the MC (i.e. the correlator) are not independent in the Markovian time, indeed the Feynman's path generated by the sweep procedure depends on the prior path, that is, the measures $C_j(t)$ have nonzero covariance in the Markovian time. In order to compute the statistical error of the average correlator $\bar{C}(t)$ We use the formula for autocorrelated variables:

$$\mathrm{var}\left(\bar{C}(t)\right) \simeq \frac{\sigma^2(C_j(t))}{\tilde{N}_s}\left(1 + 2\sum_{k=1}^{\tilde{N}_s}\frac{\Gamma(k,t)}{\Gamma(0,t)}\right) \tag{2.4.1}$$

where $\sigma^2(C_j(t))$ is the usual variance for independent (uncorrelated) variables; $\tilde{N}_s$ is a number of configurations (or sweeps) for which $\frac{\Gamma(k)}{\Gamma(0)} \simeq 0$, and the index j runs on the number

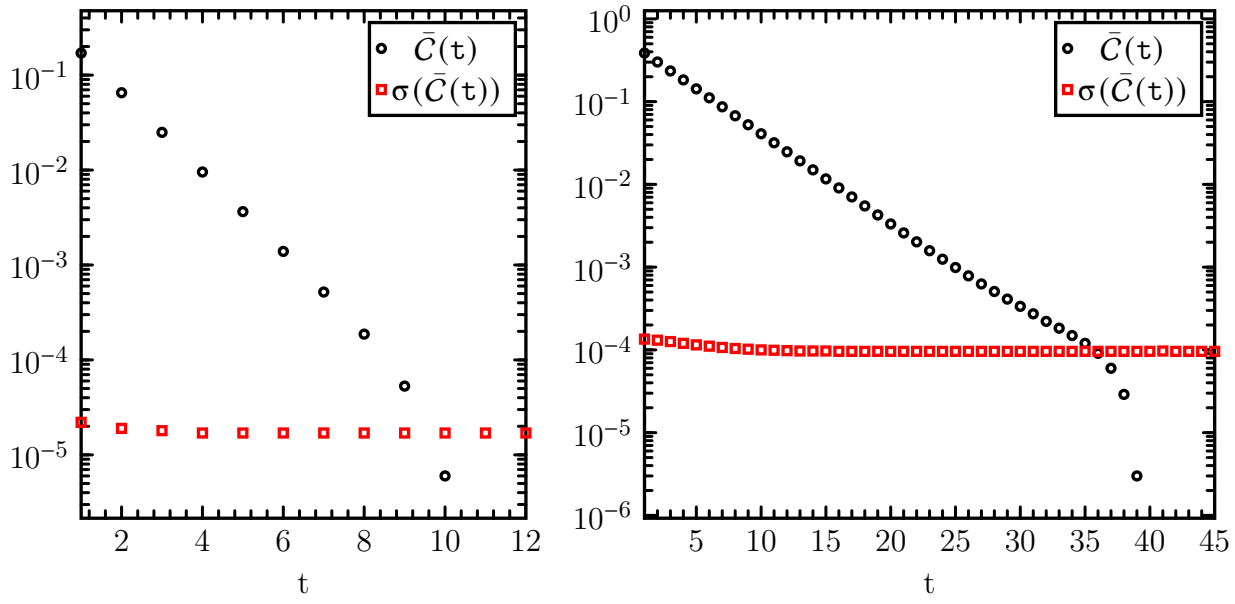

Figure 3: Averages of the correlation function (black dots) with its statistical error (red squares) for the lattice A_1 (N=64) on the left, and for the lattice A_3 (N=256) on the right.

of configurations extracted by the Metropolis: $\mathtt{j} = \{0...N_s - \tilde{N}_s\}$. The term $\Gamma(\mathtt{k},\mathtt{t})$ is the autocorrelation function of the correlator and is defined as:

$$\Gamma(\mathtt{k},\mathtt{t}) = \langle C_{\mathtt{j}}(\mathtt{t}) C_{\mathtt{j}+\mathtt{k}}(\mathtt{t})\rangle - \langle C_{\mathtt{j}}(\mathtt{t})\rangle^2 \tag{2.4.2}$$

We compute the autocorrelation function normalized to its value for $\mathtt{k} = 0$, given by the term appearing as the argument of the sum in Eq. (2.4.1). From equation (2.4.2), it can be shown that the the term in the sum in Eq. (2.4.1) behaves as an exponential of the form:

$$\frac{\Gamma(\mathtt{k},\mathtt{t})}{\Gamma(0,\mathtt{t})} \simeq e^{-\frac{\mathtt{k}}{\tau_{\mathtt{M}}}} \tag{2.4.3}$$

where $\tau_{\mathtt{M}}$ is called the decorrelation time and $\mathtt{k}$ denotes the Markovian time dependence. This result allows standard statistical analysis to be carried out, avoiding the complications induced by the autocorrelation in error calculation.

After computing the terms (2.4.2) We perform an exponential fit of the form of Eq. (2.4.3) from which the characteristic decorrelation time $\tau_{\mathtt{M}}$ is extracted; the numerical results obtained for the lattice A_2 are shown in fig 4 in the next sub-section. A "binning" procedure is carried out, which consists of averaging the MC variables $C_{\mathtt{j}}(\mathtt{t})$ over a number of configurations equal to $\sim 10\tau_{\mathtt{M}}$. In this way, the new variable averaged over the non-independent configurations can be considered as non-autocorrelated in Markovian time, and the latter is considered as the new variable of the MC. The number of independent configurations generated by the MC is given by $N_{bin} = N_s/D_{bin}$, where D_{bin} is precisely the number of configurations over which $C_{\mathtt{j}}(\mathtt{t})$ is averaged.

We henceforth refer to the "binned" variables with the notation used previously for the "unbinned" variables: $C_{\mathtt{j}}(\mathtt{t})$. After the binning procedure We recalculate the autocorrelation function using the formula (2.4.2) (where now the indices $\mathtt{j},\mathtt{k}$ run on the number of

independent configurations extracted from the MC) and We check that it is comparable with zero for $\mathtt{t}_\mathtt{M} > 0$, as shown in the right-hand side of figure 2 for the lattice A_1. We choose to analyze the autocorrelation function for $\mathtt{t} = 1$. In figure 3 the average correlator $C(\mathtt{t})$ with its statistical error is shown, computed after the binning procedure.

2.5 Numerical setup

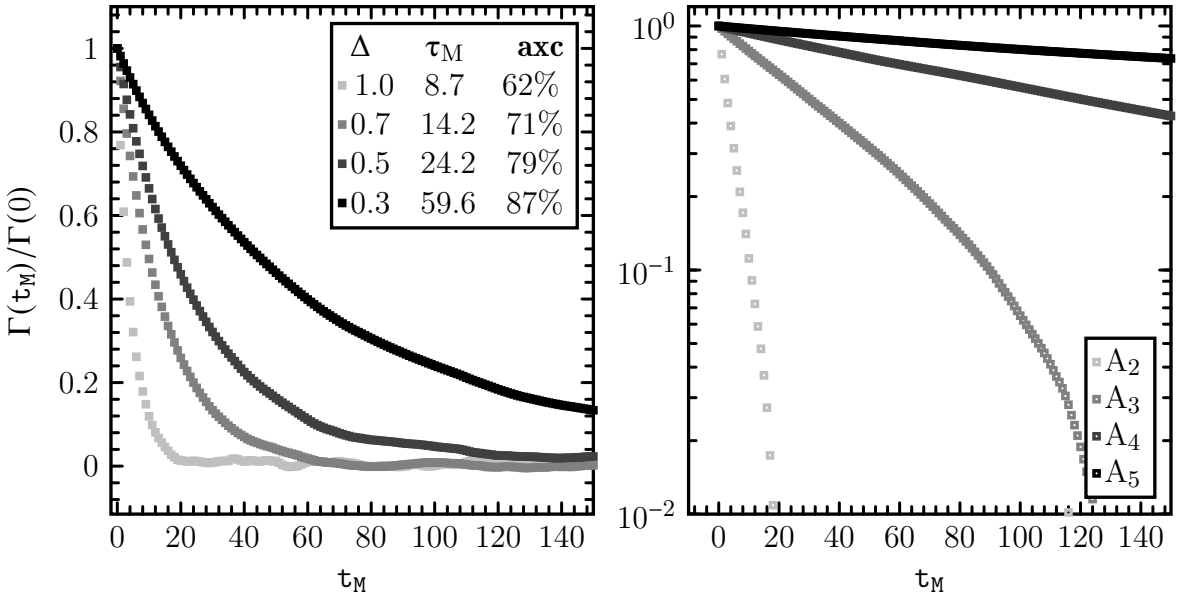

Figure 4: On the left the autocorrelation computed for the lattice A_2 for different values of Δ. On the right the autocorrelation computed for the series of lattices A_1, A_3, A_4, A_5 in logarithmic scale. $\mathtt{t}_\mathrm{M}$ stand for the Markovian time.

The parameters of the MC are summarized in table 1 for the simulations on the series of lattices $\{A_1, A_2, A_3, A_4, A_5\}$. The choice of the parameter Δ is of fundamental importance in two respects, as it influences the acceptance rate of the MA, but also determines the typical autocorrelation time τ_M of the two-point correlation function.

As anticipated in sections 2.3-2.4, the choice of Δ must be such that it ensures the efficiency of the algorithm in terms of the acceptancy, avoiding to obtain too high decorrelation times that make many of the measurements obtained from the simulation ineffective due to autocorrelation.

Figure 4 shows how different values of Δ affect the decorrelation time for the lattice A_2 on the left, while on the right the autocorrelation for the different lattices used in simulations is shown. We choose to use values of Δ that gives the lower autocorrelation times without falling below an acceptance of $\sim 60\%$.

Lattice	$\mathtt{a}$	$\mathtt{N}$	cnfg	$\mathtt{N}_{bin}$	$\mathtt{D}_{bin}$	τ_{M}	Δ	axc
A_1	1	64	1×10^8	2×10^6	50	4.5	1	68%
A_2	5×10^{-1}	128	7.5×10^7	5×10^5	150	14.2	0.7	72%
A_3	2.5×10^{-1}	256	4×10^7	1×10^5	400	41.1	0.6	68%
A_4	1.25×10^{-1}	512	4×10^7	4×10^4	1000	107.3	0.5	63%
A_5	6.25×10^{-2}	1024	6×10^7	1.5×10^4	4000	415.8	0.4	59%

Table 1: Parameters of the MC: the lattice spacing $\mathtt{a}$, the number of points in the lattice N, N_s are the generated configurations, N_{bin} is the number of bins, D_{bin} is the bin size, τ_{M} is the decorrelation time, axc is the acceptance rate (averaged over N_s sweeps).

2.6 The exponential problem

The variance of the correlator can be computed, using the P.I. formalism, as a generic physical observable:

$$\begin{aligned}\langle x_{\mathtt{l}}^2 x_{\mathtt{k}}^2\rangle - \langle x_{\mathtt{l}} x_{\mathtt{k}}\rangle^2 &= \frac{1}{\mathrm{Tr}[\hat{\mathrm{T}}_{\mathtt{a}}^{\mathrm{N}}]}\mathrm{Tr}[\hat{\mathrm{T}}_{\mathtt{a}}^{\mathrm{N}-|\mathtt{l}-\mathtt{k}|}\hat{x}^2\hat{\mathrm{T}}_{\mathtt{a}}^{|\mathtt{l}-\mathtt{k}|}\hat{x}^2] \\ &\simeq |\langle\tilde{\mathrm{E}}_0|\hat{x}^2|\tilde{\mathrm{E}}_0\rangle|^2 + e^{-|\mathtt{l}-\mathtt{k}|\mathtt{a}\Delta\tilde{\mathrm{E}}_{01}}|\langle\tilde{\mathrm{E}}_0|\hat{x}^2|\tilde{\mathrm{E}}_0\rangle|^2,\end{aligned} \tag{2.6.1}$$

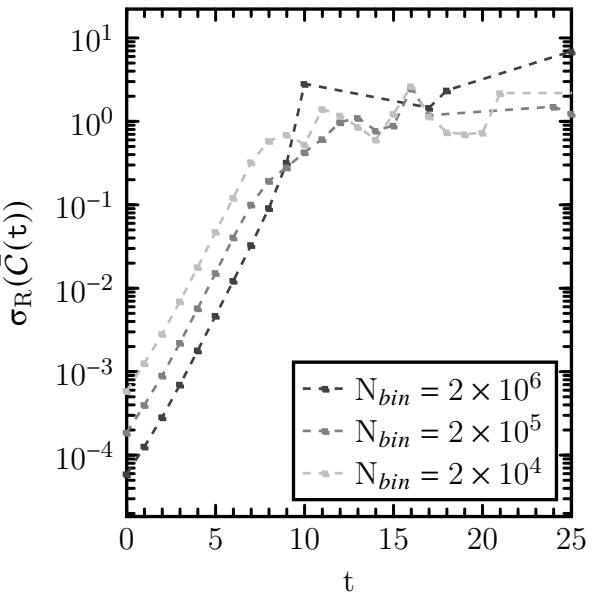

Figure 5: Relative error of $\bar{C}(\mathtt{t})$ for the lattice A_1 as the configurations generated by the MC vary. σ_{R} denotes the relative error.

where from the first to the second line the limit where $|\mathtt{l}-\mathtt{k}| \ll \frac{\mathrm{N}}{2}$ was used. Taking the limit of $|\mathtt{l}-\mathtt{k}| \gg 1$ the leading contribution in the expression (2.6.1) is given by $|\langle\tilde{\mathrm{E}}_0|\hat{x}^2|\tilde{\mathrm{E}}_0\rangle|^2$. The statistical error $\sigma(\bar{C}(t))$ reaches a plateau as the distance in physical time increases. Furthermore, it can be shown that in the limit of $|\mathtt{l}-\mathtt{k}| \ll \frac{\mathrm{N}}{2}$ the relative error of the average correlator is given by:

$$\frac{\sigma(\bar{C}(\mathtt{t}))}{\bar{C}(\mathtt{t})} \simeq \frac{1}{\sqrt{\mathrm{N}_{bin}}}\frac{\langle\tilde{\mathrm{E}}_0|\hat{x}^2|\tilde{\mathrm{E}}_0\rangle}{|\langle\tilde{\mathrm{E}}_0|\hat{x}|\tilde{\mathrm{E}}_1\rangle|^2}e^{a|\mathtt{l}-\mathtt{k}|\Delta\tilde{\mathrm{E}}_{01}}. \tag{2.6.2}$$

The result (2.6.2) is obtained by expanding the correlator in Eq. (1.4.4) as in (1.4.5). Thus, measures of the correlator for fairly large time distances cannot be used in the data analysis because of the exponential problem discussed. This feature is also evident in figure 3. Figure 5 graphs the relative errors of the average correlator for the lattice A_1; as expected, these increase with lowering the configurations generated by the MC.

3 Physics results

The estimates obtained for the correlators $\bar{C}(t)$ with $t = \{1, ..., \frac{N}{2} - 1\}$ in the previous section are used to compute the estimates of the physical observables:

$$\begin{aligned} \Delta\tilde{E}_{01}(t) &= f_1\left(\bar{C}(t-1), \bar{C}(t), \bar{C}(t+1)\right) \\ |\tilde{x}_{01}|^2(t) &= f_2\left(\bar{C}(t), \Delta\tilde{E}_{01}(t)\right) \end{aligned} \tag{3.0.1}$$

where the t dependence of the observables was introduced, since for each distance in physical time the equations (1.5.1) and (1.5.2) represent a stand-alone estimate of the energy gap and the matrix element respectively. In figure 6 are graphed the values of the observables as the distance in physical time varies, for the lattices A_1 and A_5. It can be seen that the measurements of the observables at different time distances reflects the expected plateau trend, before beginning to oscillate randomly, due to the exponential problem discussed before.

We now want to provide the best estimate of the physical observables measured on the lattice, using the values found at different physical time distances. We use the estimator:

$$\Theta(\theta, \xi) = \frac{\sum_t \bar{\theta}(t)\xi(t)}{\sum_t \xi(t)}, \tag{3.0.2}$$

which corresponds to a weighted average of the measurements, in which the weight is given by the inverse of the variance:

$$\xi(t) = \frac{1}{\sigma^2(\bar{\theta}(t))}. \tag{3.0.3}$$

The index t in Eq. (3.0.2) denotes the measures for which $\sigma_R(\bar{\theta}(t)) < 0.3$[8], which can be considered statistically significant and by this criterion are considered in the estimation of $\Theta = \{\langle\Delta\tilde{E}_{01}\rangle, \langle|\tilde{x}_{01}|^2\rangle\}$, here We use angle brackets to indicate the best estimation of the observables. The estimates thus found for the physical observables are given in table 2.

3.1 Errors analysis

The values of $C_j(t)$ extracted from the MC have nonzero covariance in the physical time distance t, since they are computed for different t from the same Feynman's path. Calculation of statistical errors of $\Delta\tilde{E}_{01}$ and $|\tilde{x}_{01}|^2$ would involve to access the covariances between $\bar{C}(t+1), \bar{C}(t), \bar{C}(t-1)$. To avoid the complications induced by this procedure, the Jackknife method is used for error estimation. We define the Jackknife cluster $\{\theta^j\}_{j=0...K-1}$ as the ensemble of the K variables θ^j defined as:

$$\theta^j = \bar{\theta} - \frac{1}{K-1}\left(\theta_j - \bar{\theta}\right), \tag{3.1.1}$$

where $\bar{\theta}$ is the average of θ_j, while the variance of $\bar{\theta}$ is:

$$\sigma^2(\bar{\theta}) = \frac{K-1}{K}\sum_{j=0}^{K-1}\left(\theta^j - \bar{\theta}\right)^2. \tag{3.1.2}$$

[8] Again with σ_R the relative error is denoted.

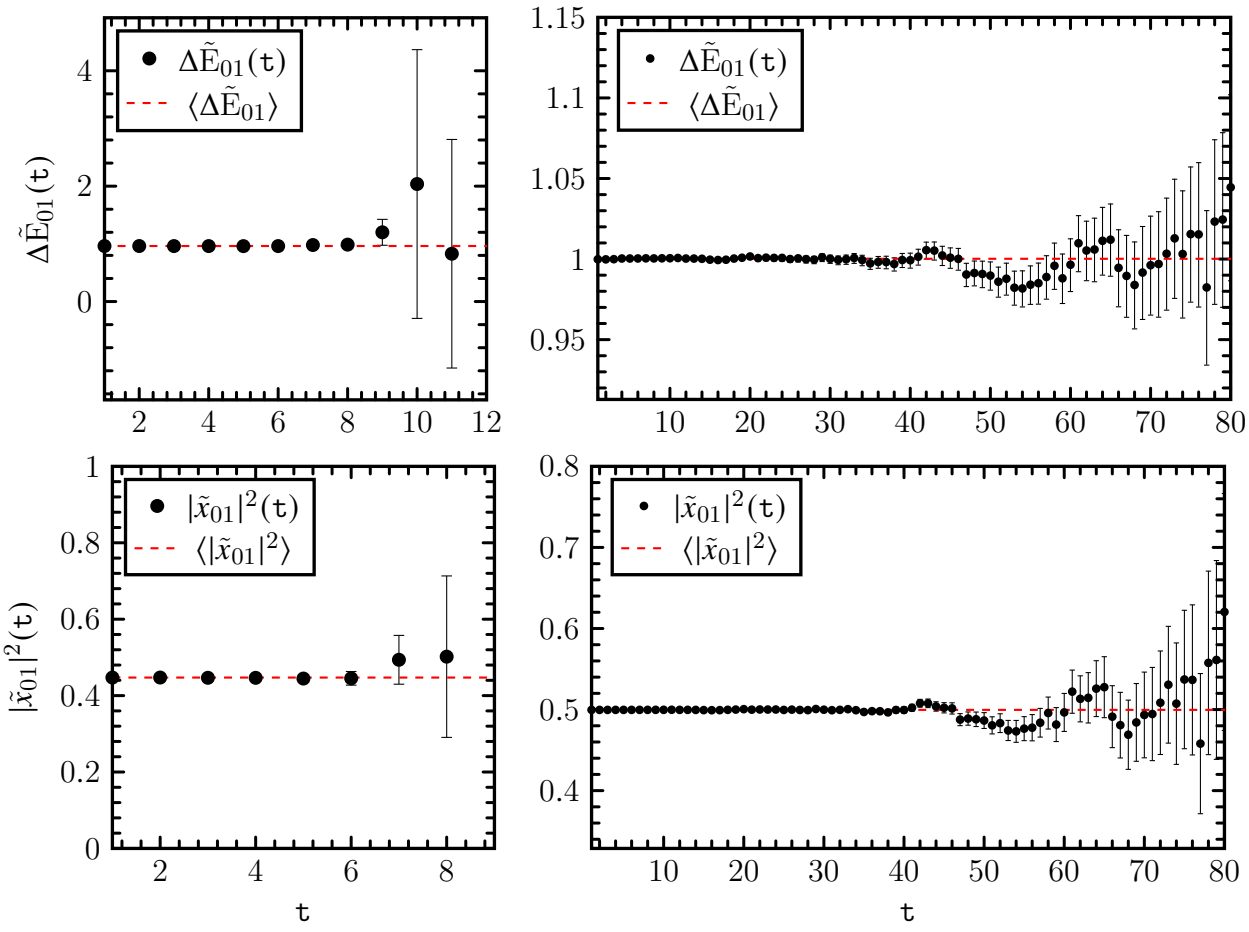

Figure 6: Above: the energy gap measurements and their errors for lattices A_1 and A_5. Below: the square of the matrix element between the first excited state and the ground state for the same lattices.

We create $\frac{N}{2} - 1$ (since the minimum t is 1) groups of measures or clusters, one for each distance in the physical time t, and We use the definition (3.1.1) to construct the Jackknife variables $C^j(t)$, where the Jackknife index $j = \{0, ..., N_{bin} - 1\}$ runs on the Markovian time (i.e. on the number of independent configurations extracted by the MC) while $\bar{\theta}$ is substituted with $\bar{C}(t)$, obtained in the previous sections. We compute the Jackknife variables for the matrix element and the energy gap as:

$$\begin{aligned} \Delta\tilde{E}^j_{01}(t) &= f_1\left(C^j(t-1), C^j(t), C^j(t+1)\right) \\ \{|\tilde{x}_{01}|^2\}^j(t) &= f_2\left(C^j(t), \Delta\tilde{E}^j_{01}(t)\right) \end{aligned} \tag{3.1.3}$$

where f_1 and f_2 are (again) the relations presented in Eq. (1.5.1) and (1.5.2) respectively. Finally, equation (3.1.2) is used to compute the statistical errors of $\Delta\tilde{E}_{01}(t)$ and $|\tilde{x}_{01}|^2(t)$. Figure 6 shows that the values of the energy gap and the matrix element have increasing error bars as the distance in physical time increases, as an effect of the exponential problem discussed in section 2.5.

In order to compute the error on the estimates of the observables (Θ) We again use

the Jackknife procedure, to avoid error propagation, which still needs the knowledge of the covariances between the estimates of the observables at different physical time distances. The Jackknife variable is constructed:

$$\Theta^{j} = f_3(\theta^{j}, \xi) \tag{3.1.4}$$

where f_3 is the definition of the estimator in Eq. (3.0.2) where We substitute $\bar{\theta}(t)$ with the corresponding jackknife variables $\theta^{j}(t)$ in Eq. (3.1.3) for the matrix element and energy gap respectively. Finally We again use the definition (3.1.2) to compute the statistical errors. The results are shown in table 2 and compared with the exact results on the lattice given by equations (1.3.3) and (1.3.4). We note that in the calculation of the error on Θ the weights associated with each measure $\bar{\theta}(t) = \{\Delta\tilde{E}_{01}(t), |\tilde{x}_{01}|^2(t)\}$ are considered without errors and treated as parameters.

Lattice	$\langle\Delta\tilde{E}_{01}\rangle$	$t(\langle\Delta\tilde{E}_{01}\rangle)$	$\langle\|\tilde{x}_{01}\|^2\rangle$	$t(\langle\|\tilde{x}_{01}\|^2\rangle)$
A_1	0.962337(78)	1.10	0.447241(27)	0.98
A_2	0.98999(13)	0.96	0.485015(55)	1.02
A_3	0.99714(28)	0.99	0.49625(13)	0.91
A_4	0.99976(47)	0.68	0.49895(22)	0.36
A_5	1.00017(70)	0.48	0.49963(32)	0.38

Table 2: Physical observables obtained from the different simulations; $t(\chi)$ is the t-student variable defined as: $t(\chi) = \chi - \chi^{th}/\sigma(\chi)$, where $\chi = \{\Delta\tilde{E}_{01}, |\tilde{x}_{01}|^2\}$.

4 Continuum limit

In order to obtain the numerical results of the physical observables in the limit of the continuum, a polynomial fit is performed between the results of the simulations on the various lattices, which are not correlated since generated from different MC. The interpolating polynomial is chosen by looking at the behavior of the physical observables on the lattice in the limit in which a tends to zero. From the equations (1.3.3) and (1.3.4) using the Taylor expansion around $a = 0$ We obtain:

$$\begin{aligned} \tilde{\omega} &= 1 - \frac{1}{24}a^2 + \frac{3}{640}a^4 + O(a^5), \\ |\langle\tilde{E}_0|\hat{x}|\tilde{E}_1\rangle|^2 &= \frac{1}{2} - \frac{1}{16}a^2 + \frac{3}{256}a^4 + O(a^5); \end{aligned} \tag{4.0.1}$$

for this reason We decide to use a linear combination of even powers of a^2 as the function to perform the fit.

$$f(a) = \alpha + \beta a^2 + \gamma a^4 \tag{4.0.2}$$

The estimates obtained for the parameters α, β and γ through the fit to the continuum are compared with the theoretical results obtained from the expansions in Eq. (4.0.1) and are given in table 3. The values of χ^2/dof obtained from the fit are 0.96 for ΔE_{01} and 0.50 for $|\langle E_0|\hat{x}|E_1\rangle|^2$. In the case of the matrix element, by restricting the fit to the values of the

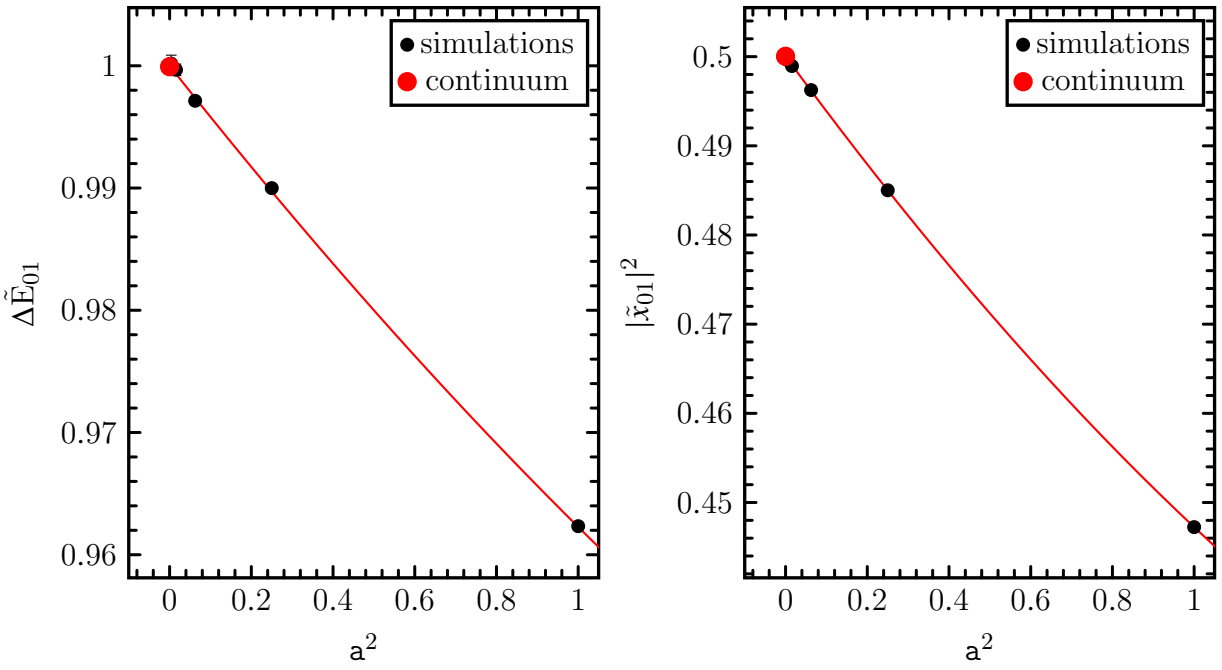

Figure 7: Observables calculated from the 5 simulations considered for continuum extrapolation. Error bars are smaller than the solid dots.

observables on the series of lattices $\{A_1, ..., A_4\}$ yields values of χ^2/dof of 0.69; We consider these as the best results in this work[9].

χ	ΔE_{01}	$\lvert x_{01}\rvert^2$	$t(\Delta E_{01})$	$t(\lvert x_{01}\rvert^2)$
α	$9.9993(29) \times 10^{-1}$	$5.0007(14) \times 10^{-1}$	0.25	0.47
β	$-4.05(17) \times 10^{-2}$	$-6.265(80) \times 10^{-2}$	0.67	0.19
γ	$2.95(1.43) \times 10^{-3}$	$9.83(67) \times 10^{-3}$	1.22	2.81

Table 3: Estimation of fit parameters; $t(\chi)$ is the t-student variable defined as: $t(\chi) = \chi - \chi^{th}/\sigma(\chi)$, where $\chi = \{\Delta E_{01}, |x_{01}|^2\}$.

The observables in the limit of the continuum are extrapolated from the fit by evaluating (4.0.2) in $a = 0$ and their error reduces to those on the parameters α. Acceptable estimates are obtained for the parameters α and β with a t-student of order 1 for the energy gap and the matrix element, while the parameter γ has a higher t-students; in the case of the energy gap σ extrapolated from fit is of the same order of the measure itself, while for the matrix element is one order of magnitude lower. The parameter γ of the matrix element is ~ 3 standard deviations from the theoretical value of the continuum. Nonetheless values found for α and β reproduce within 1 σ those of (4.0.1). Extrapolation to the continuum gives for

[9]Using also data from lattice A_5 increases the dof of the fit, without significantly increasing the value of χ^2.

the observables and their errors the results:

$$\begin{aligned} \Delta E_{01} &= 0.99993(29), \\ |x_{01}|^2 &= 0.50007(14). \end{aligned} \tag{4.0.3}$$

The values in (4.0.3) are compared with theoretical results of the continuum shown in section 1, calculating the t-student variable as shown in the first row of table 3.

5 Conclusions

MC methods prove to be a fundamental tool in the study of quantum mechanical theories, allowing access to results that cannot be obtained by perturbative methods[10]. Developing all the MC framework for a simple quantum mechanical system, as in this case, is extremely instructive because the procedure is (in theory) the same as that used to simulate relativistic quantum field theories such as quantum chromodynamics (QCD), which finds in lattice QCD the only method to investigate its non-perturbative regime (other computational methods are used in these simulations such as the hybrid MC algorithm).

6 Appendix

In this section We refer to the codes used to implement the described algorithms, which are attached to this paper.

6.1 Notation

The expression of the action in Eq. (1.2.2) is implemented numerically without explicitly introducing lattice spacing a into the formulas. In particular, We chose to make the substitutions $a\omega = \Omega$ and $\frac{m}{a} = M$, thus making the action on the lattice rewrites

$$\mathcal{S}_E = \frac{M}{2} \sum_{t=0}^{N-1} \left\{ (x_{t+1} - x_t)^2 + \Omega^2 x_t^2 \right\}. \tag{6.1.1}$$

The form above is used for the action in the discussion of numerical checks in the following sub-sections.

6.2 Action numeric check

In the implementation of the Monte Carlo method, the value of the action S determines, through its variation, the Boltzmann probability associated with a given Feynman path generated by Monte Carlo, and consequently the acceptance or rejection of the proposed path change. We present the numerical check method that ensures the correct implementation of

[10] An example is given for the theory of the an-harmonic oscillator in the strong coupling regime in the additive relation

the formula for calculating $\mathcal{S}$ that exploits the convergence properties of geometric series. We initialize the path x_t of the particle such that:

$$x_{t+1} = q x_t \tag{6.2.1}$$

where $t = \{0, ..., N-2\}$ is the physical time and $|q| < 1$ is the reason for the geometric succession; with this prescription We rewrite the action by breaking it into the kinetic and potential contributions

$$\mathcal{S}_g(x_0, q) = \frac{M}{2}(q-1)^2 \sum_{t=0}^{N-2} x_t^2 + \frac{M}{2}\left(x_N - x_{N-1}\right)^2 + \frac{M\Omega^2}{2}\sum_{t=0}^{N-1} x_t^2, \tag{6.2.2}$$

where the term in the sum corresponding to $t = N-1$ was written separately since between the first element of the lattice $x_N = x_0$ and the last x_{N-1} the relation (6.2.1) does not hold. The sums in Eq. (6.2.2) are partial geometric series of reason q^2 with partial sums given by:

$$S_K = \sum_{i=1}^{K} x_i^2 = x_0^2\left(\frac{1-q^{2K}}{1-q^2}\right). \tag{6.2.3}$$

We rewrite the action in Eq (6.1.1) using the result (6.2.3) which is compared with the result returned by the routine "**azione.c**":

$$\mathcal{S}_g(x_0, q) = \frac{M}{2}(q-1)^2 S_{N-1} + \frac{M}{2}\left(x_N - x_{N-1}\right)^2 + \frac{M\Omega^2}{2} S_N. \tag{6.2.4}$$

The implementation of the check code is executed in the main program "**check_azione.c**" which uses the routines "**geometrize_T.c**" and "**geometrize_V.c**" in the folder "**devel**"; these routines separately calculate the kinetic and potential contribution in Eq (6.2.2). The results obtained through Eq (6.2.4) reproduce those obtained through the implementation of Eq (6.1.1) for different of M and Ω, using different values for q and x_0.

6.3 Variation of the action numeric check

The routine "**dazione.c**" is used to compute the variation of the action due to the change of a single coordinate of the Feynman's path; it is called from the routine "**sweep.c**", and it represent the core of the importance sampling technique used in the MC algorithm in this work. The variation of the action computed after the change in one of the coordinates of the path is given by:

$$\delta\mathcal{S}_E = \frac{M}{2}(x_t^{new} - x_t)\left[(2+\Omega^2) - 2\left(x_{t+1} + x_{t-1}\right)\right]. \tag{6.3.1}$$

Although, in the routine that implements $\delta\mathcal{S}_E$ is preferred to use a more explicit computation that divides the kinetic and the potential contributions. In order to check the correctness of the computation We use the routine "**azione.c**" (which was previously checked) to calculate the numerical value of the action before and after the change in the t-th component of the path, separating the kinetic and the potential contributions, and check that the routine "**dazione.c**" returns the same result. Again the check is performed for different configurations of M, Ω, x_0 and q.

References

[1] M. Creutz, B. Freedman, *A statistical approach to Quantum Mechanics*, 1981, ANNALS OF PHYSICS 132, 427-462.